PHILOSOPHICAL TRANSACTIONS A

rsta.royalsocietypublishing.org

Research

Article submitted to journal

Subject Areas:
applied mathematics, geometry, theoretical physics

Keywords:
Hamiltonian dynamics, surfaces, gravity

Author for correspondence:
David G. Dritschel
e-mail:
david.dritschel@st-andrews.ac.uk

Point mass dynamics on spherical hyper-surfaces

David G. Dritschel[1]

[1]Mathematical Institute, University of St Andrews, St Andrews KY16 9SS, UK

The equations of motion are derived for a system of point masses on the (hyper-)surface $\mathbb{S}^n$ of a sphere embedded in $\mathbb{R}^{n+1}$ for any dimension $n>1$. Due to the symmetry of the surface, the equations take a particularly simple form when using the Cartesian coordinates of $\mathbb{R}^{n+1}$. The constraint that the distance of the jth mass $\|\boldsymbol{r}_j\|$ from the origin remains constant (i.e. each mass remains on the surface) is automatically satisfied by the equations of motion. Moreover, the equations are a Hamiltonian system with a conserved energy as well as a host of conserved angular momenta. Several examples are illustrated in dimensions $n=2$ (the sphere) and $n=3$ (the glome).

1. Introduction

The dynamics of point masses on general closed surfaces (focusing primarily on surfaces of revolution) was recently discussed in [2], extending analogous results for point vortices in [7]. Herein, the focus is on spherically-symmetric surfaces but for any dimension n, in particular (hyper-)surfaces $\mathbb{S}^n$ embedded in $\mathbb{R}^{n+1}$ for $n>2$.

The key assumption in [2] is that (Newtonian) gravity is a central force. The gravitational potential can then be determined by analogy with Maxwell's formulation of electrostatics. (For historical background, the reader may wish to consult [4], [2] and [8], the latter in this issue). Moreover, the dynamical equations can be derived from the expressions of kinetic and potential energy using the metric of the surface. This leads to a Hamiltonian system with conserved "energy" — the total kinetic plus potential energy, excluding the infinite self-energy of each point mass. In addition, due to the rotational symmetry of the surface, there are $n(n+1)/2$ conserved components of the angular momenta.

THE ROYAL SOCIETY PUBLISHING

While $\mathbb{S}^n$ is embedded in $\mathbb{R}^{n+1}$, the potential is not found from Poisson's equation in $\mathbb{R}^{n+1}$, but rather from the corresponding Laplace-Beltrami equation restricted to $\mathbb{S}^n$. This profoundly affects the nature of the dynamics, and leads to the peculiar requirement that the total mass on $\mathbb{S}^n$ must integrate to zero. In particular, any positive point masses must be *compensated*. Here this is done by a uniform negative mass distributed across $\mathbb{S}^n$.

This paper is organised as follows. In the next section, the derivation of the equations governing point mass dynamics on the sphere $\mathbb{S}^2$ first stated in [2] are briefly reviewed. These are then extended to $\mathbb{S}^n$, making use of the appropriate Green function satisfying the Gauss condition of $\mathbb{S}^n$, namely that the surface integral of the Laplace-Beltrami operator (the Laplacian of $\mathbb{R}^{n+1}$ restricted to $\mathbb{S}^n$) vanishes. It is shown that the resulting equations conserve total energy as well as a host of angular momenta. In section 3, numerical simulations are used to illustrate the dynamics of a pair of masses on both the sphere $\mathbb{S}^2$ and the "glome" $\mathbb{S}^3$. Conclusions are offered in section 4.

2. The equations of motion

(a) The sphere $\mathbb{S}^2$

On a sphere, Stokes' theorem requires that the surface integral of the mass distribution vanishes identically. This is known as the "Gauss condition" (see [2] or [7] for details). This is a peculiar condition for a mass distribution, as it requires any positive mass to be compensated by negative mass. Nevertheless, it is a mathematical constraint for any closed surface. In the analogous vortex dynamics problem [7], there is nothing special about negative vorticity, and the formulation of the dynamics poses no conceptual difficulties.[1] In the mass problem, there is no escape from having negative mass. The simplest solution is to distribute the negative mass *uniformly* to compensate the positive mass, here concentrated in points.

In both the mass and vortex problem, this leads to a modification of the Green function expressing the potential of a unit point mass or point circulation. For an open surface, the Green function can be obtained by a conformal transformation from the surface to the plane $\mathbb{R}^2$. However, this is not enough for a closed surface. The Green function is modified so that a unit point mass or circulation is compensated by a uniform negative value spread across the surface. In this way, the Green function incorporates the Gauss condition. If this is not done, the bare Green function has two antipodal singularities and is, in effect, the solution to Poisson's equation for *two* opposite-signed anti-podal delta-function sources (Dirac measures) [5].

It should be stressed that the Green function is obtained from the Laplace-Beltrami operator *on the surface* (intrinsic), not from the Laplace operator in the embedding space (extrinsic). In other words, the surface alone is the entire space under consideration. For example, mass dynamics restricted to a plane in $\mathbb{R}^3$ is not the same as mass dynamics in $\mathbb{R}^2$; the Green functions differ. This changes fundamental aspects of the two-body (Kepler) problem, as discussed in [2,4] and references therein.

In [7], the construction of the Green function on $\mathbb{S}^2$ incorporating the Gauss condition was shown to lead to the governing equations for point vortices first derived in [6]. These equations used the Cartesian coordinates of $\mathbb{R}^3$ constrained to $\mathbb{S}^2$, i.e. $\|\boldsymbol{r}_j\| = 1$ for each point vortex j on a unit sphere. The equations in Cartesian coordinates are particularly simple and exploit the isotropy of the surface.

In [2], an analogous Cartesian formulation of the equations for point mass dynamics was presented. The key result is that the gravitational potential in the mass problem has the same form as the streamfunction in the vortex problem. This allows one to carry over results from the vortex problem to the mass problem, whose principle difference is that the potential gives rise to the acceleration field rather than the velocity field. The equations also follow directly from the

[1] Likewise, the dynamics of point charges pose no such difficulties, and the equations derived below apply equally well to point charges moving on $\mathbb{S}^n$.

general formulation presented in [2]. For a collection of N masses $m_1, m_2, \ldots, m_N$ located on a unit sphere at $\boldsymbol{r}_1(t), \boldsymbol{r}_2(t), \ldots, \boldsymbol{r}_N(t)$ where t is time, they read

$$\begin{aligned} \dot{\boldsymbol{r}}_k &= \boldsymbol{v}_k \\ \dot{\boldsymbol{v}}_k &= \frac{1}{4\pi} \sum_{j \neq k} m_j \frac{\boldsymbol{r}_j - (\boldsymbol{r}_j \cdot \boldsymbol{r}_k)\boldsymbol{r}_k}{1 - \boldsymbol{r}_j \cdot \boldsymbol{r}_k} - \|\boldsymbol{v}_k\|^2 \boldsymbol{r}_k, \end{aligned} \tag{2.1}$$

where a dot denotes a time derivative. Here, the gravitational constant is taken to be unity, without loss of generality. One can verify that the identity

$$\frac{d}{dt}(\boldsymbol{r}_k \cdot \boldsymbol{v}_k) = \dot{\boldsymbol{r}}_k \cdot \boldsymbol{v}_k + \boldsymbol{r}_k \cdot \dot{\boldsymbol{v}}_k = 0 \tag{2.2}$$

is satisfied, as required. This follows from the constraint $\boldsymbol{r}_k \cdot \boldsymbol{r}_k = 1$ (and thus $\boldsymbol{r}_k \cdot \boldsymbol{v}_k = 0$), i.e. that the masses remain on the unit sphere. Notably, a single mass moves at constant speed v on a great circle because $\boldsymbol{v}_1 \cdot \dot{\boldsymbol{v}}_1 = 0$ from (2.1) when $N = 1$ (and the sum is absent).

The total (kinetic plus potential) energy H, the Hamiltonian of the system, is obtained from

$$H = \frac{1}{2} \sum_{k=1}^{N} m_k |\boldsymbol{v}_k|^2 + \frac{1}{2\pi} \sum_{k=2}^{N} \sum_{j=1}^{k-1} m_j m_k \ln \|\boldsymbol{r}_j - \boldsymbol{r}_k\| \tag{2.3}$$

and is a constant of motion. Significantly, the potential part involves the Green function of $\mathbb{R}^2$, namely $(2\pi)^{-1} \ln r$, where $r = \|\boldsymbol{r}_j - \boldsymbol{r}_k\|$ is the chord distance between masses j and k (see [6]). Since all masses lie on the unit sphere, r^2 can also be written $2(1 - \boldsymbol{r}_j \cdot \boldsymbol{r}_k)$.

In addition, three components of the angular momentum are conserved:

$$\boldsymbol{A} = \sum_{k=1}^{N} m_k \boldsymbol{r}_k \times \boldsymbol{v}_k. \tag{2.4}$$

This follows from the rotational symmetry of the surface and may be deduced from (2.1). These are independent first integrals, so provide three constraints on the dynamics: they reduce the available degrees of freedom by three, just as in the corresponding point vortex problem of $\mathbb{S}^2$ [10]. Another constraint comes from conservation of energy H and a further from the invariance of the equations of motion to the time-varying coordinate transformation $\varphi_k \to \varphi_k + \nu t$ where φ_k is the longitude of mass k, see [2]. This effectively reduces the system to $4N - 5$ degrees of freedom. A canonical reduction of the Hamiltonian system in [4] for $N = 2$ masses also finds 3 effective degrees of freedom.

Hamilton's equations — with the added constraint that the masses remain on the surface — may be used to deduce (2.1) from the Hamiltonian H in (2.3), *extended* to include N Lagrange multipliers $\lambda_1, \lambda_2, \ldots, \lambda_N$ chosen to ensure that the masses remain on the surface:

$$H_e = H + \sum_{k=1}^{N} \lambda_k (\boldsymbol{r}_k \cdot \boldsymbol{r}_k - 1). \tag{2.5}$$

The equations of motion are then found from Hamilton's equations

$$\begin{aligned} m_k \dot{\boldsymbol{r}}_k &= \frac{\partial H_e}{\partial \boldsymbol{v}_k} = m_k \boldsymbol{v}_k \\ m_k \dot{\boldsymbol{v}}_k &= -\frac{\partial H_e}{\partial \boldsymbol{r}_k} = \frac{m_k}{4\pi} \sum_{j \neq k} m_j \frac{\boldsymbol{r}_j}{1 - \boldsymbol{r}_j \cdot \boldsymbol{r}_k} - 2\lambda_k \boldsymbol{r}_k. \end{aligned} \tag{2.6}$$

Next, the Lagrange multipliers are determined by enforcing the constraint (2.2):

$$m_k \|\boldsymbol{v}_k\|^2 + \frac{m_k}{4\pi} \sum_{j \neq k} m_j \frac{\boldsymbol{r}_j \cdot \boldsymbol{r}_k}{1 - \boldsymbol{r}_j \cdot \boldsymbol{r}_k} - 2\lambda_k = 0.$$

Solving for the λ_k and inserting them into (2.6) leads directly to (2.1) after dividing both equations in (2.6) by m_k.

The Poisson bracket of the Hamiltonian system may be conveniently expressed in the Cartesian coordinates and velocities. For two quantities $\mathcal{F}$ and $\mathcal{G}$ (normally first integrals like H or $\boldsymbol{A}$, see below), we have

$$\{\mathcal{F},\mathcal{G}\} \equiv \sum_{j=1}^{N} \frac{1}{m_j} \sum_{\alpha=1}^{n+1} \frac{\partial \mathcal{F}}{\partial r_{j\alpha}} \frac{\partial \mathcal{G}}{\partial v_{j\alpha}} - \frac{\partial \mathcal{F}}{\partial v_{j\alpha}} \frac{\partial \mathcal{G}}{\partial r_{j\alpha}}, \tag{2.7}$$

where $r_{j\alpha}$ denotes the α component of $\boldsymbol{r}_j$, and similarly for $v_{j\alpha}$. Here $n=2$ is the dimension of the surface. The dynamical equations (2.1) may then be written $\dot{\boldsymbol{r}}_k = \{\boldsymbol{r}_k, H_e\}$ and $\dot{\boldsymbol{v}}_k = \{\boldsymbol{v}_k, H_e\}$. Conservation of angular momentum is implied by $\{A_\alpha, H_e\} = 0$ for each component α. Moreover the angular momentum components satisfy the (degenerate) cyclic relations $\{A_1, A_2\} = A_3$, $\{A_2, A_3\} = A_1$ and $\{A_3, A_1\} = A_2$, showing that each pair generates the remaining component. A set of first integrals are said to be in involution if their Poisson bracket vanishes. This occurs only for the set H_e, $\|\boldsymbol{A}\|^2$ and any component of the angular momentum, say A_3, just as in the analogous point vortex problem [10].

(b) Hyper-spheres $\mathbb{S}^n$ for $n > 2$

The result above for the sphere $\mathbb{S}^2$ is now generalised to hyper-spheres $\mathbb{S}^n$ in higher dimensions n. The equations follow from the extended Hamiltonian, just as above for $n=2$. All that is required, then, is the expression for potential energy. For this, we need the Green function of the Laplace-Beltrami operator, i.e. the solution to

$$\Delta G = \delta(\boldsymbol{\varphi} - \boldsymbol{\varphi}_o) - \frac{1}{S_n} \tag{2.8}$$

where S_n is the surface "area" of $\mathbb{S}^n$, and $\boldsymbol{\varphi} = (\varphi_1, \varphi_2, \ldots, \varphi_n)$ are the surface angular coordinates ($\boldsymbol{\varphi}_o$ refers to the source point) related to Cartesian coordinates in $\mathbb{R}^{n+1}$ via

$$\begin{aligned} r_1 &= \cos\varphi_1 \\ r_2 &= \sin\varphi_1 \cos\varphi_2 \\ &\ldots\ \ldots \\ r_n &= \sin\varphi_1 \ldots \sin\varphi_{n-1} \cos\varphi_n \\ r_{n+1} &= \sin\varphi_1 \ldots \sin\varphi_{n-1} \sin\varphi_n \end{aligned} \tag{2.9}$$

(see [1]). All angles range from 0 to π except φ_n which ranges from 0 to 2π. Note: r_1 is the axial (or z) coordinate on $\mathbb{S}^2$.

Due to the isotropy of $\mathbb{S}^n$, the Green function can only depend on the angle θ between two points $\boldsymbol{r}$ and $\boldsymbol{r}_o$ (with angular coordinates $\boldsymbol{\varphi}$ and $\boldsymbol{\varphi}_o$ respectively), i.e. $\cos\theta = \boldsymbol{r}\cdot\boldsymbol{r}_o$. If the source point is placed at the "north pole" $\varphi_{1o} = 0$, then θ reduces to φ_1. Then (2.8) simplifies considerably to

$$\frac{1}{\sin^{n-1}\theta} \frac{d}{d\theta}\left(\sin^{n-1}\theta \frac{dG}{d\theta}\right) = \delta(\theta) - \frac{1}{S_n}. \tag{2.10}$$

The general solution is

$$G(\theta) = -\frac{1}{S_{n-1}} \int_\theta^{\pi/2} \frac{d\theta'}{\sin^{n-1}\theta'} + \frac{1}{S_n} \int_\theta^{\pi/2} \frac{d\theta'}{\sin^{n-1}\theta'} \int_0^{\theta'} \sin^{n-1}\theta'' d\theta''. \tag{2.11}$$

The first integral has singularities at both $\theta = 0$ and π, while the second has a singularity at $\theta = \pi$ which cancels the first. The pre-factor S_{n-1} in front of the first integral follows by applying Gauss' theorem to the first integral over a vanishingly small surface surrounding $\theta = 0$ (see [5]). Note: $S_{n-1} = 2\pi^{n/2}/\Gamma(n/2)$ where Γ is the gamma function [9].

For the sphere $\mathbb{S}^2$, the first integral gives

$$\frac{1}{4\pi}\ln\left(\frac{1-\cos\theta}{1+\cos\theta}\right)$$

while the second gives

$$\frac{1}{4\pi}\ln\left(\frac{1+\cos\theta}{2}\right)$$

whose sum is

$$G(\theta)=\frac{1}{4\pi}\ln\left(\frac{1-\cos\theta}{2}\right),$$

which is the Green function for $\mathbb{S}^2$ (see [7] for details). Using $r=\|\boldsymbol{r}-\boldsymbol{r}_o\|=\sqrt{2(1-\cos\theta)}$, then G is seen to be the Green function for $\mathbb{R}^2$, $(2\pi)^{-1}\ln r$, plus an unimportant constant. This coincidence only happens when $n=2$.

For $\mathbb{S}^n$, $G(\theta)$ can be found by straightforward integration. For $n=3$, the "glome", illustrated in the next section, we find

$$G(\theta)=-\frac{\cot\theta}{4\pi}\left(1-\frac{\theta}{\pi}\right). \tag{2.12}$$

This may be readily verified by differentiation, and satisfies the requirement that it is only singular as $\theta\to 0$, i.e. it satisfies the Gauss condition. Moreover, for $\theta\ll 1$, this asymptotes to the Green function for $\mathbb{R}^3$, namely $-1/(4\pi r)$. In one higher dimension, $n=4$, we find

$$G(\theta)=\frac{1}{8\pi^2}\left(\ln(1-\cos\theta)-\frac{1}{1-\cos\theta}\right). \tag{2.13}$$

Again, this may be readily verified and is singular only as $\theta\to 0$. Moreover, for $\theta\ll 1$, this asymptotes to the Green function for $\mathbb{R}^4$, namely $-1/(4\pi^2r^2)$.[2]

Given the Green function, the potential energy P takes the form

$$P=\sum_{k=2}^{N}\sum_{j=1}^{k-1}m_jm_kG(\theta_{jk}) \tag{2.14}$$

where $\cos\theta_{jk}=\boldsymbol{r}_j\cdot\boldsymbol{r}_k$. The kinetic energy K takes the same form in all dimensions, hence the Hamiltonian (total energy) for mass motion on $\mathbb{S}^n$ is given by

$$H=\frac{1}{2}\sum_{k=1}^{N}m_k|\boldsymbol{v}_k|^2+\sum_{k=2}^{N}\sum_{j=1}^{k-1}m_jm_kG(\theta_{jk}). \tag{2.15}$$

As before, the Hamiltonian must be extended just as in (2.5) to ensure that the masses remain on $\mathbb{S}^n$. Applying Hamilton's equations

$$m_k\dot{\boldsymbol{r}}_k=\frac{\partial H_e}{\partial\boldsymbol{v}_k}\quad\&\quad m_k\dot{\boldsymbol{v}}_k=-\frac{\partial H_e}{\partial\boldsymbol{r}_k}$$

and the constraint (2.2) then yields the final form of the equations of motion:

$$\begin{aligned}\dot{\boldsymbol{r}}_k&=\boldsymbol{v}_k\\ \dot{\boldsymbol{v}}_k&=\sum_{j\neq k}m_j(\boldsymbol{r}_j-(\boldsymbol{r}_j\cdot\boldsymbol{r}_k)\boldsymbol{r}_k)F(\theta_{jk})-\|\boldsymbol{v}_k\|^2\boldsymbol{r}_k\end{aligned} \tag{2.16}$$

where

$$F(\theta)=\frac{1}{\sin\theta}\frac{dG}{d\theta}. \tag{2.17}$$

For $\mathbb{S}^3$, this is

$$F(\theta)=\frac{1}{4\pi\sin^3\theta}\left(1-\frac{\theta}{\pi}\right)+\frac{\cos\theta}{4\pi^2\sin^2\theta}, \tag{2.18}$$

[2]For $\mathbb{R}^n$ and $n>2$, one can use Gauss' theorem to prove that $G(r)=-1/((n-2)S_{n-1}r^{n-2})$.

while for $\mathbb{S}^4$, this is

$$F(\theta) = \frac{1}{8\pi^2}\left(\frac{1}{1-\cos\theta} + \frac{1}{(1-\cos\theta)^2}\right). \tag{2.19}$$

A plot of $F(\theta)$ and $G(\theta)$ for $\mathbb{S}^3$ is provided in figure 1, confirming they are monotonic, non-singular functions except when $\theta = 0$.

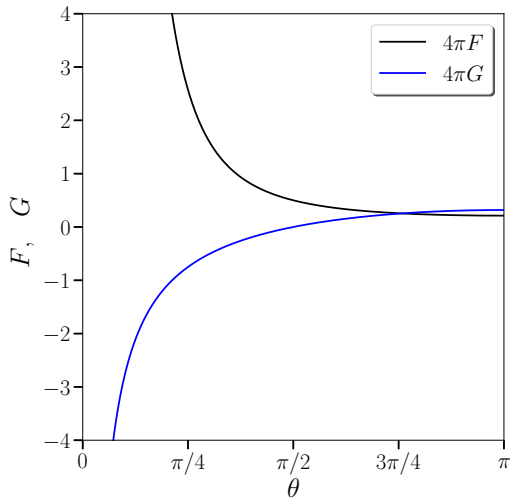

Figure 1. Forms of the functions $F(\theta)$ and $G(\theta)$ that apply to the glome $\mathbb{S}^3$. These are singular only when $\theta \to 0$. As $\theta \to \pi$, the limiting values of G and F are $1/(4\pi^2)$ and $1/(6\pi^2)$, respectively.

Besides total energy H, there are a number of angular momenta which are constants of the motion due to the rotational symmetry of the surface. In general, these may be written in the form

$$A_{\alpha\beta} = \sum_{k=1}^{N} m_k(r_{k\alpha}v_{k\beta} - r_{k\beta}v_{k\alpha}) \tag{2.20}$$

where $r_{k\alpha}$ denotes the α component of $\boldsymbol{r}_k$ (with α an integer in the range $[1, n+1]$), with similar meanings for $r_{k\beta}$, $v_{k\alpha}$ and $v_{k\beta}$. Since $A_{\alpha\alpha} = 0$ and $A_{\beta\alpha} = -A_{\alpha\beta}$, only $A_{\alpha\beta}$ for $1 \le \alpha \le n$ and $\alpha + 1 \le \beta \le n + 1$ are unique and non-zero. These reduce to the forms given by the vector cross product in (2.4) when $n = 2$.

The Poisson bracket $\{\mathcal{F}, \mathcal{G}\}$ is the same as given in (2.7), and one can show that $\{A_{\alpha\beta}, A_{\alpha'\beta'}\} = \delta_{\alpha\alpha'}A_{\beta\beta'} - \delta_{\beta\alpha'}A_{\alpha\beta'}$, where $\delta_{\alpha\beta}$ is the usual Kronecker delta symbol. Here it suffices to take $\alpha \in [1, n-1]$, $\alpha' \in [\alpha, n]$ as well as $\beta \in [\alpha+1, n+1]$ and $\beta' \in [\alpha'+1, n+1]$ to cover all distinct cases. The Poisson bracket is therefore zero only when all indices differ. For $n = 3$, the brackets $\{A_{12}, A_{34}\}$, $\{A_{13}, A_{24}\}$ and $\{A_{14}, A_{23}\}$ all vanish, while there are four cyclic groups $\{A_{12}, A_{13}\} = A_{23}$ (with the two other permutations), $\{A_{12}, A_{14}\} = A_{24}$, $\{A_{13}, A_{14}\} = A_{34}$ and $\{A_{23}, A_{24}\} = A_{34}$. One may show that H_e, the 'Casimirs' $C_1 \equiv A_{12}^2 + A_{13}^2 + A_{14}^2 + A_{23}^2 + A_{24}^2 + A_{34}^2$ and $C_2 \equiv A_{12}A_{34} - A_{13}A_{24} + A_{14}A_{23}$, and the pair A_{13} and A_{24} are in involution. By a canonical reduction of the Hamiltonian for 2 masses on $\mathbb{S}^3$, [4] prove that there are 3 effective degrees of freedom. For $N \ge 2$ masses, this is expected to be $6N - 9$ effective degrees of freedom. In general, on $\mathbb{S}^n$, it is conjectured that there are $2n(N-2) + 3$ effective degrees of freedom.

3. Illustration of the dynamics of two masses

Numerical codes in python were written to study point mass dynamics on both $\mathbb{S}^2$ and $\mathbb{S}^3$. The dopri5 (mixed 4th and 5th-order Runge-Kutta) method with adaptive time stepping was used

to ensure high accuracy, in particular for near collisions. In the examples below, the total energy and all angular momenta are conserved to around one part in 10^6. (The codes are available on request.)

(a) The sphere $\mathbb{S}^2$

Here just one example involving two masses of unequal size is provided for illustration. A full exploration of the large parameter space is beyond the scope of this paper. The example provided already indicates rich behaviour, which is likely to be chaotic in general [4].

We start with two masses $m_1 = 4\pi$ and $m_2 = 2\pi$. The longitude of the first mass ϕ_1 is taken to be zero while its co-latitude θ_1 is taken to be $\pi/4$. For the second mass, we take $\phi_2 = \pi/3$ and $\theta_2 = 3\pi/4$. To specify the initial velocities, we take $\dot\phi_1 = 0$, $\dot\theta_1 = 0$, $\dot\phi_2 = 2$ and $\dot\theta_2 = 1$. (Note: in terms of the angle coordinates $\boldsymbol{\varphi}$ introduced for a general surface $\mathbb{S}^n$ in the previous section, we have $\theta = \varphi_1$ and $\phi = \varphi_2$, see (2.9).)

The evolution from $t = 0$ to 50 is summarised in figure 2, which shows the r_1 (or axial) coordinate of each mass, the speed of each mass, the distance between them, and their angular rotation frequency Ω. The latter is computed from

$$\Omega = \frac{\|(\boldsymbol{r}_2 - \boldsymbol{r}_1) \times (\boldsymbol{v}_2 - \boldsymbol{v}_1)\|}{\|\boldsymbol{r}_2 - \boldsymbol{r}_1\|^2}.$$

Despite the isotropy of the surface, the two masses appear to exhibit an irregular, possibly chaotic orbit, with periods of close approach characterised by rapid rotation (note the $\log_{10}$ scaling of Ω in the bottom panel). Much longer integrations (not shown) do not suggest that the evolution is periodic. A Poincaré section could be used to examine chaotic motion, as in [4], but this is left to a future work. It is likely however that chaotic behaviour is generic, as the number of effective degrees of freedom is 3 for two masses [2,4].

Conservation of energy and angular momentum are examined in figure 3, where additionally the kinetic and potential energies, K and P, are shown. Note that over the time period shown, the masses travel more than 112 times the radius of the sphere. There is a near perfect cancellation of the variations in K and P, as required for the total energy $H = K + P$ to be conserved. Likewise, the magnitude of the angular momentum $\|\boldsymbol{A}\|$ remains well conserved. The total energy variation is less than 6×10^{-7} of the mean and less than 2.3×10^{-7} of the maximum kinetic energy, while the magnitude of the angular momentum variation is less than 3×10^{-7} of the mean.

(b) The glome $\mathbb{S}^3$

We next turn to mass dynamics[3] on the glome, $\mathbb{S}^3$. Again we illustrate just one example involving two masses of unequal size. We start with two masses $m_1 = 4\pi$ and $m_2 = 2\pi$. We specify the positions $\boldsymbol{r}_k$ using the "surface" angles φ_{k1}, φ_{k2} and φ_{k3} via

$$\begin{aligned} r_{k1} &= \cos\varphi_{k1} \\ r_{k2} &= \sin\varphi_{k1}\cos\varphi_{k2} \\ r_{k3} &= \sin\varphi_{k1}\sin\varphi_{k2}\cos\varphi_{k3} \\ r_{k4} &= \sin\varphi_{k1}\sin\varphi_{k2}\sin\varphi_{k3} \end{aligned} \tag{3.1}$$

for each mass k (see (2.9) and [1]).

The initial angles are taken as follows: $\varphi_{11} = \pi/2$, $\varphi_{12} = \pi/4$, $\varphi_{13} = 0$, $\varphi_{21} = \pi/6$, $\varphi_{22} = 5\pi/6$ and $\varphi_{23} = \pi/2$. The initial velocities are specified through the rates of change of these angles. We take $\dot\varphi_{11} = 0$, $\dot\varphi_{12} = 0$, $\dot\varphi_{13} = 0$, $\dot\varphi_{21} = 1$, $\dot\varphi_{22} = -1$ and $\dot\varphi_{23} = 1/2$.

The evolution from $t = 0$ to 50 is summarised in figure 4, which shows the axial coordinate of each mass r_{k1}, the speed of each mass, the distance between them, and their angular rotation

[3] Alternative formulations of the dynamics, not using the Green function derived here, can be found in [3].

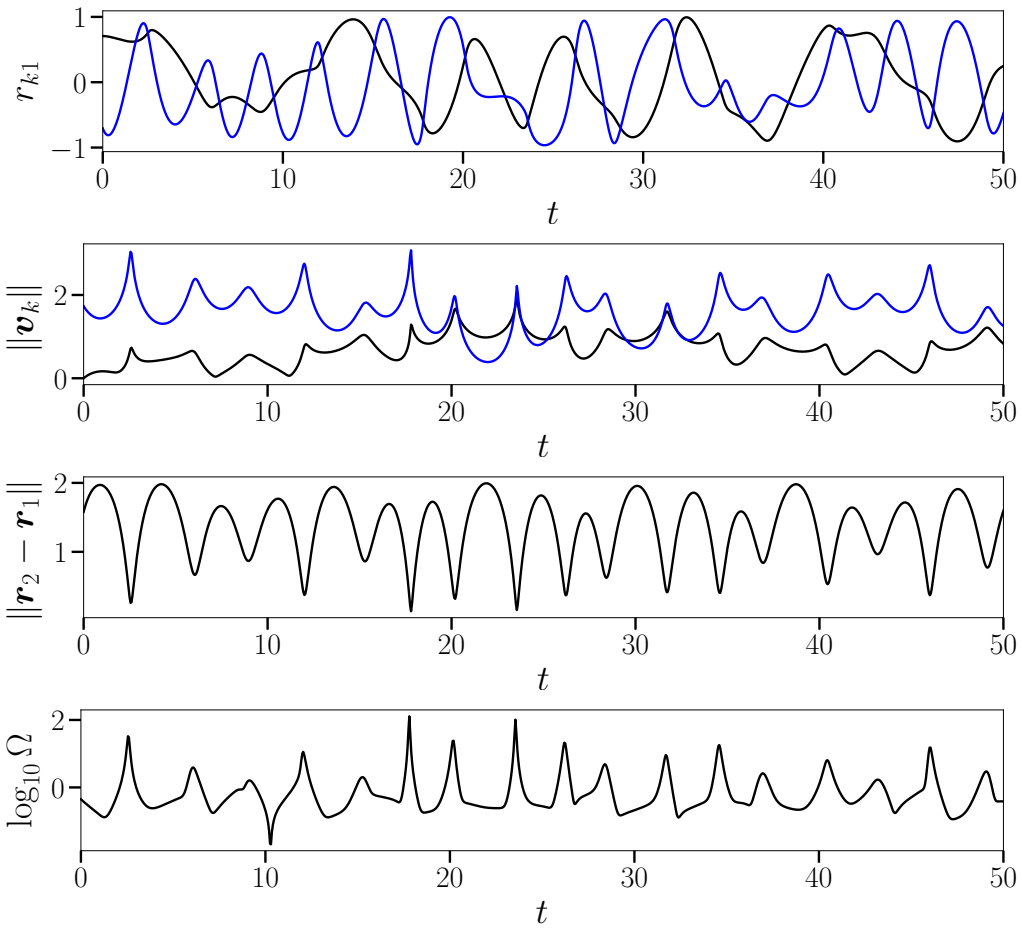

Figure 2. Properties of the interaction of two unequal masses on a sphere $\mathbb{S}^2$. The top panel shows the axial coordinate of each mass (the first in black, the second in blue). The second panel shows the speed $\|\boldsymbol{v}_k\|$ of each mass with the same colouring scheme. The third panel shows the distance $\|\boldsymbol{r}_2 - \boldsymbol{r}_1\|$ between the masses, and the fourth shows the angular rotation speed Ω of the two masses (see text for definition).

frequency Ω. The latter is computed from

$$\Omega = \frac{\left[\sum_{\alpha=1}^{3}\sum_{\beta=\alpha+1}^{4}(r_{1\alpha}v_{2\beta} - r_{2\beta}v_{1\alpha})^2\right]^{1/2}}{\|\boldsymbol{r}_2 - \boldsymbol{r}_1\|^2}.$$

As in the case of the sphere $\mathbb{S}^2$, the two masses exhibit an irregular, possibly chaotic orbit, with periods of close approach characterised by rapid rotation (note the $\log_{10}$ scaling of Ω). Again, much longer integrations do not suggest that the evolution is periodic, and in general the motion is expected to be chaotic as the number of effective degrees of freedom is 3, just as in the case of $\mathbb{S}^2$ [4].

Conservation of energy and angular momentum are examined in figure 5. In this case, the masses travel more than 77 times the radius of the glome over the time period shown. Again the kinetic and potential energies, K and P, are shown to demonstrate near perfect cancellation, as required for the total energy $H = K + P$ to be conserved. Likewise, the magnitude of the angular

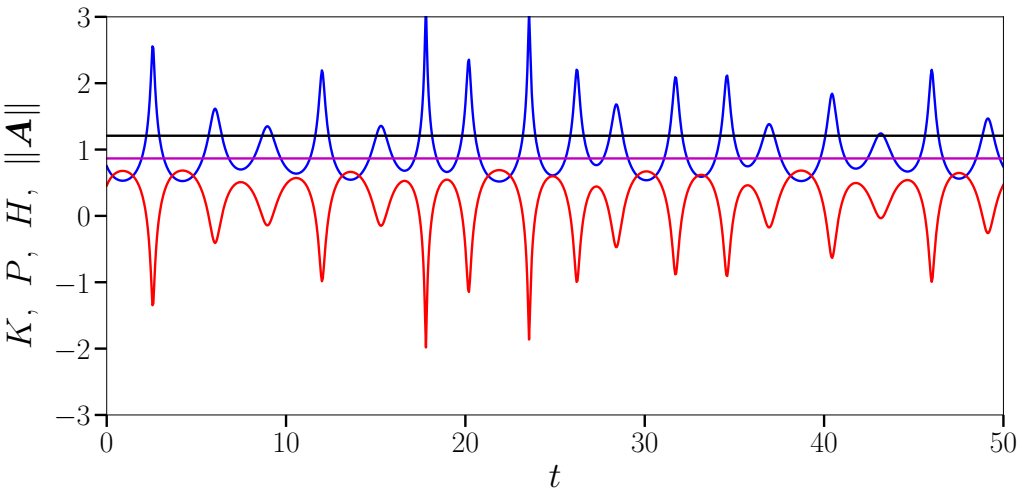

Figure 3. Evolution on $\mathbb{S}^2$ of the kinetic and potential energies, K (blue) and P (red), together with the total energy $H = K + P$ (black) and magnitude of the angular momentum $\|\boldsymbol{A}\|$ (magenta). Note: the plotted energies are divided by 4π to compare with $\|\boldsymbol{A}\|$ on the same scale.

momentum

$$\|\boldsymbol{A}\| = \left(\sum_{\alpha=1}^{3} \sum_{\beta=\alpha+1}^{4} A_{\alpha\beta}^2 \right)^{1/2}$$

(see (2.20)) remains well conserved. The total energy variation is less than 6×10^{-6} of the mean and less than 2×10^{-7} of the maximum kinetic energy, while the magnitude of the angular momentum variation is less than 9×10^{-8} of the mean.

4. Conclusion

The equations governing point mass dynamics on spherical (hyper-)surfaces $\mathbb{S}^n$ for $n > 2$ have been derived. The key result is that the gravitational potential just depends on the form of the Green function, the solution to Poisson's equation (or the Laplace-Beltrami equation) on $\mathbb{S}^n$ which incorporates the Gauss condition, namely that the surface integral of the mass density vanishes on any closed surface. This condition cannot be relaxed: it is a mathematical requirement on any closed surface.

Equipped with the expression for potential energy and the simple form of kinetic energy, Hamilton's equations were used to derive the system of governing equations. To do this, one must supplement the Hamiltonian (the total energy) by a constraint involving Lagrange multipliers which keeps the masses on the surface.

An example considering the interaction of two unequal masses was presented for both the sphere $\mathbb{S}^2$ and the glome $\mathbb{S}^3$. In both cases, excellent conservation of total energy and angular momentum was demonstrated. The dynamics exhibited appears to be chaotic, though further work is required to clarify this.

There are many open problems. Besides chaotic motion, the basic issue of closed or open orbits (the Kepler problem) remains to be investigated. The equations present a veritable playground for mathematical exploration.

Ethics. There are no ethical considerations.

Data Accessibility. Please contact the author for the numerical codes used.

Competing Interests. The author declares that he has no competing interests.

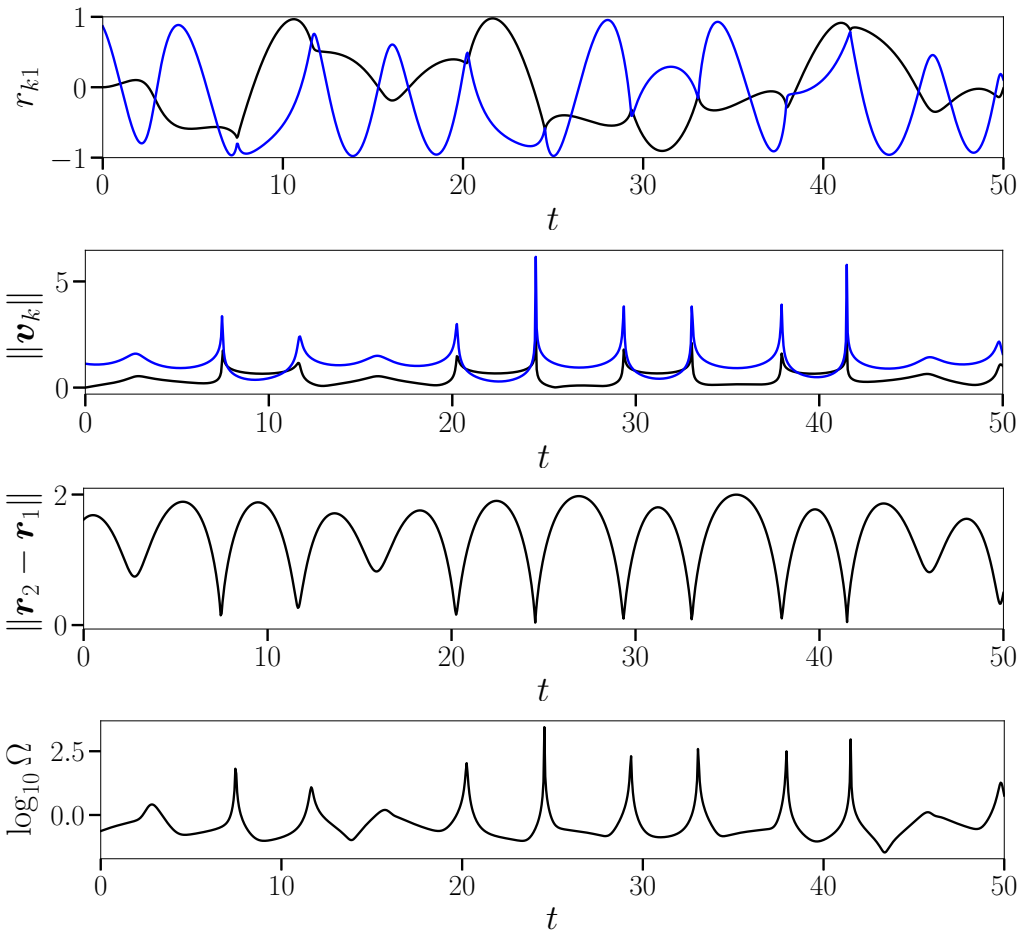

Figure 4. Properties of the interaction of two unequal masses on a glome $\mathbb{S}^3$. The top panel shows the axial coordinate r_{k1} of each mass ($k=1$ in black, $k=2$ in blue). The second panel shows the speed $\|\boldsymbol{v}_k\|$ of each mass with the same colouring scheme. The third panel shows the distance $\|\boldsymbol{r}_2 - \boldsymbol{r}_1\|$ between the masses, and the fourth shows the angular rotation speed Ω of the two masses (see text for definition).

References

1. Blumenson LE 1960. A derivation of n-dimensional spherical coordinates. *Amer. Math. Monthly* **67**, 63–66.
2. Boatto S, Dritschel DG, Schaefer RG 2016. N-body dynamics on closed surfaces: the axioms of mechanics. *Proc. R. Soc. A* **472**, 20160020.
3. Borisov AV, Mamaev IS 2006. The restricted two-body problem in constant curvature spaces. *Celestial Mech. Dyn. Astr.* **96**, 1–17.
4. Borisov AV, Mamaev IS, Bizyaev, IA 2016. The spatial problem of 2 bodies on a sphere: reduction and stochasticity. *Reg. Chaotic Dyn.* **21(5)**, 556–580.
5. Cohl HS 2011. Opposite antipodal fundamental solution of Laplace's qquation in hyperspherical geometry. *SIGMA* **7**, 108.
6. Dritschel DG 1988. Contour dynamics/surgery on the sphere. *J. Comput. Phys.* **78**, 477–483.
7. Dritschel DG, Boatto S 2015. The motion of point vortices on closed surfaces. *Proc. R. Soc. A* **471**, 20140890.
8. Falconer IJ 2019. Vortices and atoms in the Maxwellian era. *Proc. R. Soc. A* **???**, (this special issue).

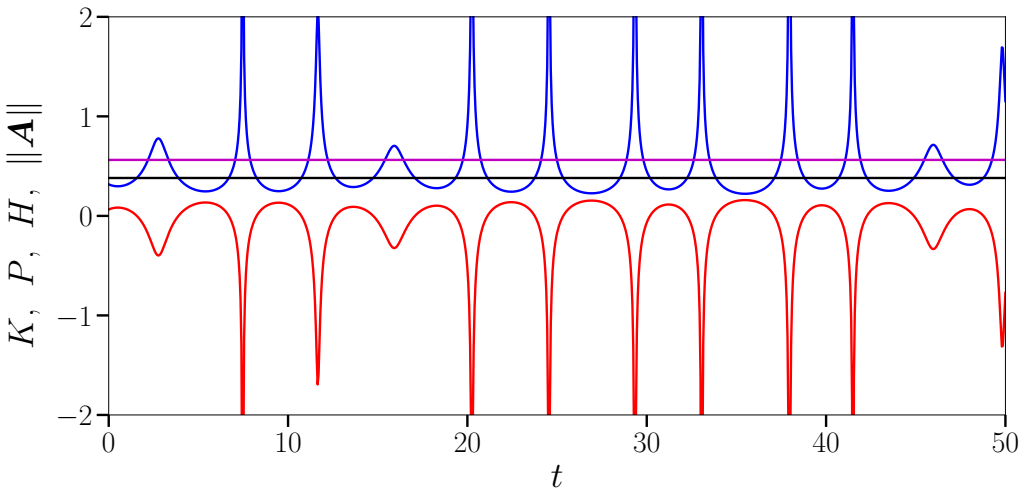

Figure 5. Evolution on $\mathbb{S}^3$ of the kinetic and potential energies, K (blue) and P (red), together with the total energy $H = K + P$ (black) and magnitude of the angular momentum $\|\boldsymbol{A}\|$ (magenta). The K and P variation is much greater than visible in this restricted plot range: the maximum K is nearly 13.59, while the minimum P is nearly -13.21. Note: the plotted energies are divided by 4π to compare with $\|\boldsymbol{A}\|$ on the same scale.

9. Loskot P 2007. On monotonicity of the hypersphere volume and area. *J. Geometry* **87**, 96–98.
10. Sakajo T 1999. The motion of three point vortices on a sphere. *Japan J. Ind. Appl. Math.* **16(3)**, 321–330.